

MODELLING OF ROTATING VERTICAL AXIS TURBINES USING A MULTIPHASE FINITE ELEMENT METHOD

Van Dang Nguyen*, Johan Jansson*[†], Massimiliano Leoni[‡], Bärbel Janssen*,
Anders Goude[‡], and Johan Hoffman*

*Department of Computational Science and Technology, School of Computer Science and
Communication, KTH Royal Institute of Technology, Stockholm, Sweden.
e-mail: {vdnguyen, jjan, barbel, jhoffman}@kth.se

[†] Basque Center for Applied Mathematics, Bilbao, Spain.
e-mail: mleoni@bcamath.org.

[‡] Uppsala University, Uppsala, Sweden.
e-mail: anders.goude@angstrom.uu.se

Key words: Vertical axis turbines, fluid-structure interaction, fluid-rigid body interaction, Unicorn solver, FEniCS-HPC, Navier-Stokes equations, multiphase finite element method.

Abstract. We combine the unified continuum fluid-structure interaction method with a multiphase flow model to simulate turbulent flow and fluid-structure interaction of rotating vertical axis turbines in offshore environments. This work is part of a project funded by the Swedish Energy Agency, which focuses on energy systems combining ecological sustainability, competitiveness and reliability of supply. The numerical methods used comprise the Galerkin least-squares finite element method, coupled with the arbitrary Lagrangian-Eulerian method, in order to compute weak solutions of the Navier-Stokes equations for high Reynolds numbers on moving meshes. Mesh smoothing methods help to improve the mesh quality when the mesh undergoes large deformations. The simulations have been performed using the Unicorn solver in the FEniCS-HPC framework, which runs on supercomputers with near optimal weak and strong scaling up to thousands of cores.

1 INTRODUCTION

Wind and water have been sources of energy for thousands of years, and one of the most utilized during the 17-th and 18-th centuries [10]. Nowadays, the increased interest in renewable energy resources has caused an increase in wind and water power utilization, and improvement of wind and hydraulic turbine technology. The function of a wind turbine is the result of a complex interaction of its components and subsystems such as the blades, rotor, tower, foundation, power train, control system, etc. [1]. Vertical axis turbines have long been used to convert kinetic energy from wind/water into electrical power, and numerical solution of the Navier-Stokes equations for simulation of wind turbines may explain some physical phenomena and

give some guidance for improvement. Simulation of a rotating turbine is a challenging problem, considered an open problem in all its complexity, even though some impressive results have been achieved using stabilized finite element methods [2, 3].

In this paper, we combine the unified continuum fluid-structure interaction method [7] with a multiphase flow model [9] to simulate turbulent flow and fluid-structure interaction of rotating turbines in offshore environments. This work is part of a project funded by the Swedish Energy Agency, which focuses on energy systems combining ecological sustainability, competitiveness and reliability of supply. The numerical method used comprises the Galerkin least-squares finite element method, coupled with the arbitrary Lagrangian-Eulerian method in order to allow us to compute weak solutions of the Navier-Stokes equations for high Reynolds numbers on moving meshes. Mesh smoothing methods help to improve the mesh quality when the mesh undergoes large deformations. The simulations have been performed using the Unicorn solver in the FEniCS-HPC framework, which runs on supercomputers with near optimal weak and strong scaling up to thousands of cores.

The paper is organized as follows. We first introduce in Section 2 the vertical axis turbine used for all simulations in the paper. In Section 3 we consider a simplified model based on fluid-rigid body interaction in which the turbine rotates with a given rotational speed applied to the computation mesh. In Section 4 we study a full fluid-structure interaction model. The computer implementation is discussed in Section 5. In Section 6 we present some preliminary results and suggest future directions.

2 A VERTICAL AXIS TURBINE

The turbine under consideration is a single 3-bladed H-rotor turbine, with a radius of 3.24 m and a blade length of 5 m (Fig. 1a, is reproduced from [5]). The blades are pitched outwards with a chord length of 0.25 m at the middle of the blade. For simplification, we assume that the turbine axis is coincident with the z -axis and that the turbine Ω^T is placed in a cylinder Ω^C (Fig. 1b)

$$\Omega^C = \{(x, y, z) \in \mathbf{R}^3 \mid x^2 + y^2 \leq R^2, z \in [-L/2; L/2]\}. \quad (1)$$

Here we choose $R = 30$ m and $L = 20$ m, with the turbine axis placed in the center-line of the cylinder domain. Let f and s indicate fluid and structure parts respectively and for fluid-structure interaction we denote $\Omega^f = \Omega^C \setminus \Omega^T$ and $\Omega^s = \Omega^T$.

3 FLUID-RIGID BODY INTERACTION MODEL

We start with a simplified model where the structure is assumed to be a rigid body, so that we remove Ω^s from the domain and solve only for the fluid domain $\Omega = \Omega^f$ where the turbine is forced to rotate with a given rotational velocity. The incompressible Navier-Stokes equations Eq. 2 need to be solved in the fluid part, $\Omega = \Omega^f$.

$$\begin{cases} \dot{\mathbf{u}} + (\mathbf{u} \cdot \nabla) \mathbf{u} - \nu \Delta \mathbf{u} + \nabla p = \mathbf{f} & \text{in } \Omega \times I \\ \nabla \cdot \mathbf{u} = 0 & \text{in } \Omega \times I \\ \mathbf{u}(\cdot, 0) = \mathbf{u}_0 & \text{in } \Omega \end{cases} \quad (2)$$

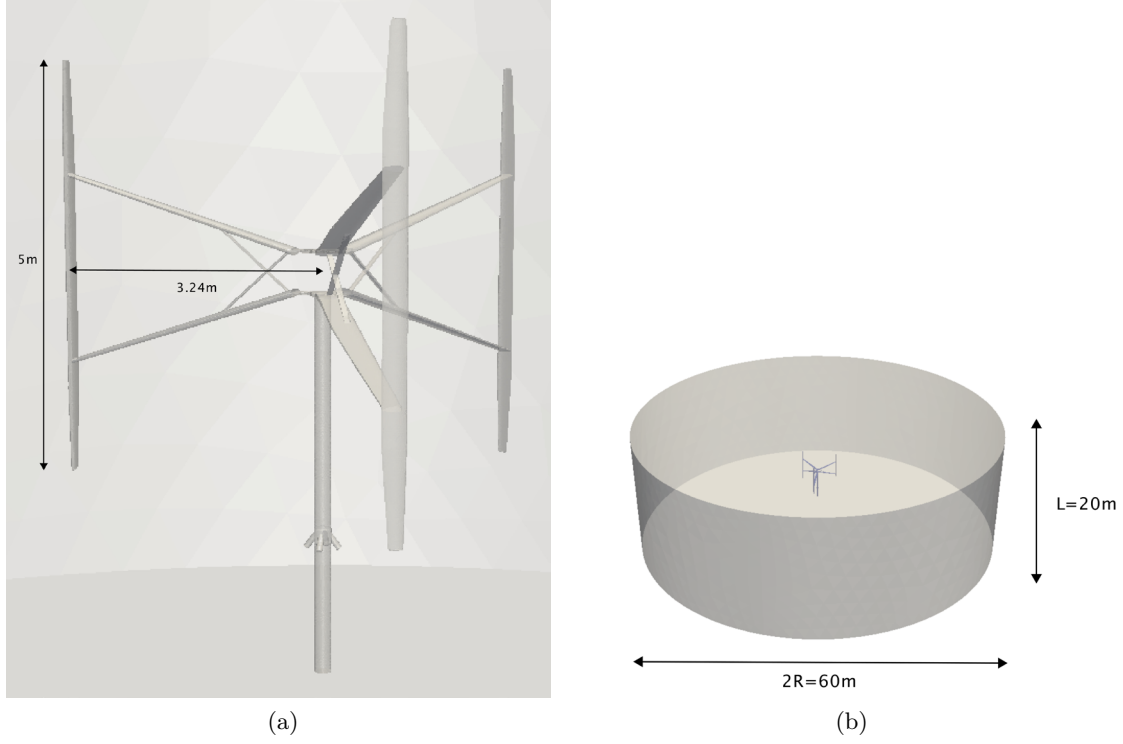


Figure 1: A vertical axis turbine reproduced from [5] (a), placed in a cylinder (b).

Here, \mathbf{u} is the unknown velocity, p is the unknown pressure, ν is the kinematic viscosity computed as the ratio between the dynamic viscosity μ and the density ρ , i.e. $\nu = \mu/\rho$, and \mathbf{f} is a given body force. Eq. (2) is subjected to the slip velocity boundary condition

$$\mathbf{u} \cdot \mathbf{n} = 0 \quad (3)$$

or the no-slip velocity boundary condition

$$\mathbf{u} = 0 \quad (4)$$

on boundary of the fluid domain at the turbine surface $\Gamma^{\mathcal{T}}$. Here \mathbf{n} is the outward unit normal of the fluid boundary and σ denotes the stress tensor.

The inflow velocity boundary condition $\mathbf{u} = (u_i, 0, 0)$ and the outflow condition $p = 0$ are imposed on Γ^i and Γ^o respectively. These boundaries are defined as follows

$$\Gamma^{\mathcal{T}} = \partial\Omega \cap \Omega^{\mathcal{T}} \quad (5)$$

$$\Gamma^i = \{x \in \partial\Omega \mid x \leq 0\} \setminus \Gamma^{\mathcal{T}} \quad (6)$$

$$\Gamma^o = \{x \in \partial\Omega \mid x > 0\} \setminus \Gamma^{\mathcal{T}} \quad (7)$$

To solve this problem, the simplest algorithm we can think of is to manually rotate the computational domain. At each time step, we update the mesh and the corresponding finite element

function spaces. However, the solution from the previous time step needs to be interpolated to the new function spaces. This process is expensive and accumulates interpolation errors. To overcome the problem, the arbitrary Lagrangian-Eulerian (ALE) method [4] is applied. This method automatically projects the solution from the previous time step to the current function space without using interpolation. The Navier-Stokes' momentum equation 2 formulated in ALE coordinates with a mesh velocity β reads

$$\dot{\mathbf{u}} + ((\mathbf{u} - \beta) \cdot \nabla) \mathbf{u} - \nu \Delta \mathbf{u} + \nabla p = \mathbf{f} \quad (8)$$

Galerkin least-squares space-time FEM [6] is used to obtain an efficient method for the discretization of a rotating turbine problems. Let $0 = t_0 < t_1 < \dots < t_N = T$ be a time partition associated with the time intervals $I_n = (t^{n-1}, t^n]$ of length $k_n = t^n - t^{n-1}$. Let $\mathbf{Q} \subset \mathbf{H}^1(\Omega)$, $\mathbf{Q}_0 \subset \mathbf{H}_0^1(\Omega)$ and $\mathbf{V} = [\mathbf{Q}_0]^d$. The ALE finite element method with least-squares stabilization is stated as the following. For all time intervals I_{n+1} , find $(U^{n+1}, P^{n+1}) \in \mathbf{V}_h \times \mathbf{Q}_h$ such that

$$\begin{aligned} & \left((U_h^{n+1} - U_h^n) k_{n+1}^{-1} + ((\hat{U}_h^n - \beta) \cdot \nabla) \hat{U}_h^n, v \right) + \left(\nu \nabla \hat{U}_h^n, \nabla v \right) - \left(P^{n+1}, \nabla \cdot v \right) \\ & + \left(\nabla \cdot \hat{U}_h^n, q \right) + SD_\delta \left(\hat{U}_h^n, P^{n+1}; v, q \right) = (f, v) \end{aligned} \quad (9)$$

where

$$\begin{aligned} SD_\delta \left(\hat{U}_h^n, P^{n+1}; v, q \right) = & \left(\delta_1 \left((\hat{U}_h^n \cdot \nabla) \hat{U}_h^n + \nabla P_h^{n+1} - f \right), (\hat{U}_h^n \cdot \nabla) v + \nabla q \right) \\ & + \left(\delta_2 \nabla \cdot \hat{U}_h^n, \nabla \cdot v \right) \end{aligned} \quad (10)$$

for all $(v, q) \in \mathbf{V}_h \times \mathbf{Q}_h$. Here δ_1 and δ_2 are stabilization parameters given by positive constants C_1 , C_2 , the time step size k_n and the mesh size h_n

$$\begin{aligned} \delta_1 &= C_1 \left(\frac{1}{k_n^2} + \frac{|U^{n-1}|^2}{h_n^2} \right)^{-1/2} \\ \delta_2 &= C_2 h_n |U^{n-1}| \end{aligned} \quad (11)$$

Since the inflow and outflow boundary conditions are not moving with the mesh, they need to be updated for each new time step.

4 FLUID-STRUCTURE INTERACTION MODEL

Including structure deformation, the rotating turbine can be described using a unified continuum fluid-structure interaction model [7]:

$$\begin{cases} \rho (\dot{\mathbf{u}} + (\mathbf{u} \cdot \nabla) \mathbf{u}) + \nabla \cdot \sigma = \mathbf{f} & \text{in } \Omega \times I \\ \nabla \cdot \mathbf{u} = 0 & \text{in } \Omega \times I \\ \dot{\theta} + (\mathbf{u} \cdot \nabla) \theta = 0 & \text{in } \Omega \times I \\ \mathbf{u}(\cdot, 0) = \mathbf{u}_0 & \text{in } \Omega \end{cases} \quad (12)$$

The computational domain is $\Omega = \Omega^f \cup \Omega^s$, $\Gamma^{fs} = \overline{\Omega^f} \cap \overline{\Omega^s}$, the phase function θ defines the structure and fluid domains

$$\theta(x, t) = \begin{cases} 1 & \text{if } x \in \Omega^f \\ 0 & \text{if } x \in \Omega^s \end{cases} \quad (13)$$

For a Newtonian fluid and an incompressible Neo-Hookean solid, the stress σ is computed as the following

$$\begin{aligned} \sigma &= -\sigma_D + p\mathcal{I} \\ \sigma_D &= \theta\sigma_f + (1 - \theta)\sigma_s \\ \sigma_f &= 2\mu_f\epsilon(\mathbf{u}) \\ \sigma_s &= 2\mu_s\epsilon(\mathbf{u}) + \nabla\mathbf{u}\sigma_s + \sigma_s\nabla\mathbf{u}^T \end{aligned} \quad (14)$$

The no-slip velocity boundary condition in this setting means that

$$\mathbf{u}_f = \mathbf{u}_s \quad (15)$$

on Γ^{fs} and the slip condition is

$$\mathbf{u}_f \cdot \mathbf{n} = \mathbf{u}_s \cdot \mathbf{n} \quad (16)$$

We also need to assure the force balance condition at the interface, i.e $\sigma_f \cdot \mathbf{n} = \sigma_s \cdot \mathbf{n}$.

The variational form of the FSI model in ALE coordinates reads

$$\begin{aligned} (\rho\dot{u}, v) + ((u - \beta) \cdot \nabla u, v) - (p, \nabla \cdot v) + (\alpha\epsilon(u), \epsilon(v)) + (\delta_1(u - \beta) \cdot \nabla u, (u - \beta) \cdot \nabla v) \\ + (\delta_2 \nabla p, \nabla q) - (\nabla \cdot u, q) = (f, v) - (1 - \theta)(\sigma_D^{n-1}, \nabla v) \end{aligned} \quad (17)$$

where v, q are test functions and

$$\begin{aligned} \rho &= \theta\rho^f + (1 - \theta)\rho^s \\ \alpha &= \theta 2\nu + (1 - \theta)kE \end{aligned}$$

Since the solid part of the mesh moves, the mesh at the interface between the solid and the fluid becomes ill conditioned. Laplacian mesh smoothing techniques have been used to redistribute the vertices of the mesh in the fluid domain. The technique works by moving all the internal vertices to the center of all its neighbors.

5 IMPLEMENTATIONS

The two numerical models described above have been implemented in Unicorn and the high performance branch of the finite element problem solving environment DOLFIN-HPC which is optimized for distributed memory architectures using a hybrid MPI+OpenMP approach with efficient parallel I/O. Both Unicorn and DOLFIN-HPC are written in C++ and the implementation has proven to be portable across several different architectures, such as ordinary Unix/Linux workstations. We use ParMETIS for mesh partitioning.

The first model has been implemented with both the slip condition (Eq. 3) and the no-slip condition (Eq. 4), whereas the second model has only been implemented with the no-slip condition in Eq. 16.

6 PRELIMINARY RESULTS AND DISCUSSION

The proposed methods were implemented in the Unicorn solver for parallel adaptive finite element simulation of turbulent flow and fluid-structure interaction. The solver showed near optimal weak and strong scaling results when simulating turbulent flow on massively parallel machines [8]. The adaptive mesh refinement in the solver, however, is disabled for this case since the h -adaptivity does not work properly for rotating computational domains. The use of r -adaptivity may be a better choice for the ALE case of rotating domain and we leave it for future works. The simulations were carried out on the Beskow supercomputer at the KTH Royal Institute of Technology, that is a Cray XC40 system, based on Intel Haswell processors and Cray Aries interconnect network. Each Beskow node has 32 cores divided into two sockets, with 16 cores each, and thus the total number of cores is 53632. The available RAM for each node is 64 GB DDR3 SDRAM.

The volume meshes were generated with ANSA from Beta-CAE Systems with 556789 vertices for the fluid part and 116622 vertices for the structure part. We note that in the fluid-rigid body interaction model, only the fluid part of the mesh is used whereas in the fluid-structure interaction model, the computational mesh unifies the fluid mesh and the structure mesh.

Numerical simulations show that the fluid-rigid body interaction model works efficiently. We show in Fig. 2 drag forces for three rotational velocities: fixed turbine, $\pi/200$ rad/s and $\pi/20$ rad/s. A larger rotational velocity gives larger oscillations. Some snapshots in time for the two

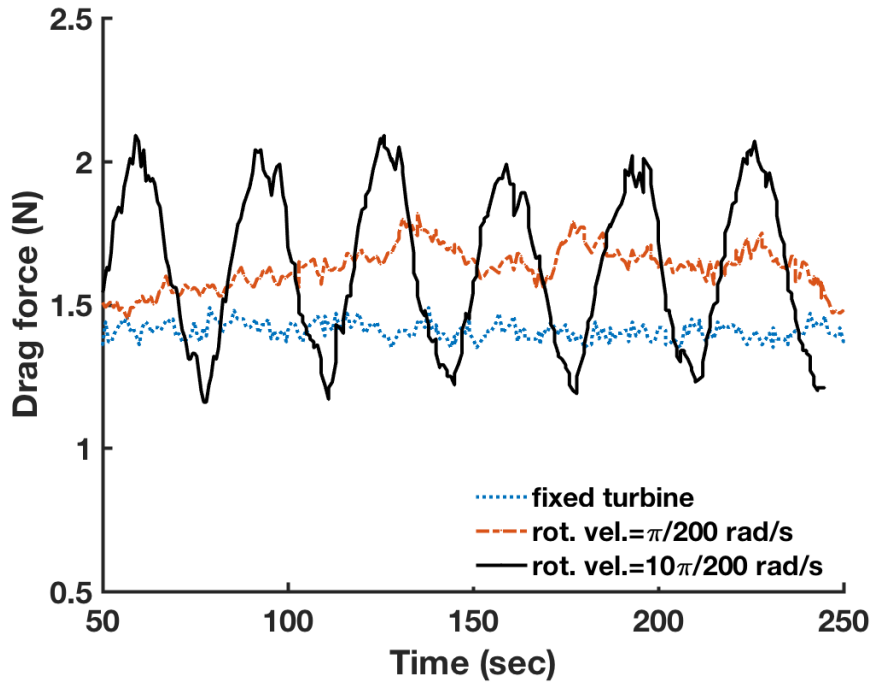


Figure 2: Drag forces for three rotational velocities: fixed turbine, $\pi/200$ rad/s and $\pi/20$ rad/s.

rotational velocities are visualized in Fig. 3 and Fig. 4 respectively.

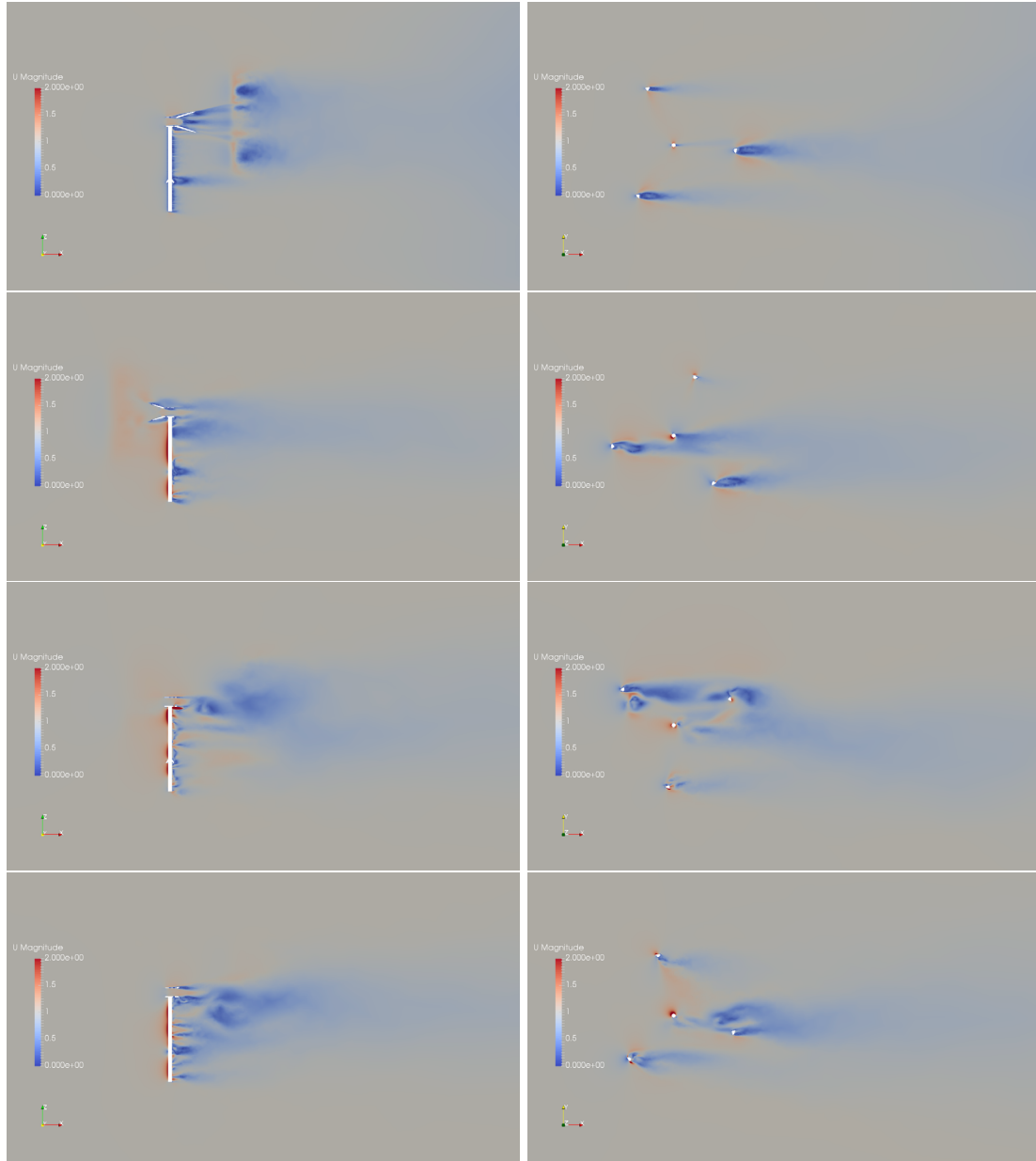


Figure 3: Rotating turbine at rotational speed $\pi/200$ rad/s , for 4 snapshots in time: horizontal cuts (left) and vertical cuts (right).

Fig. 5a shows a vertical cut of the computed velocity for the fluid-structure interaction model where the no-slip velocity Eq. 15 is applied. Under the effect of the inflow velocity, the turbine rotates for a while (Fig. 5b) before stopping in the position shown in Fig. 5c. One of the reasons may be because the no-slip boundary condition (15) is not suitable. A Nitsche method for the slip condition (16) is under consideration and it is expected to solve the problem.

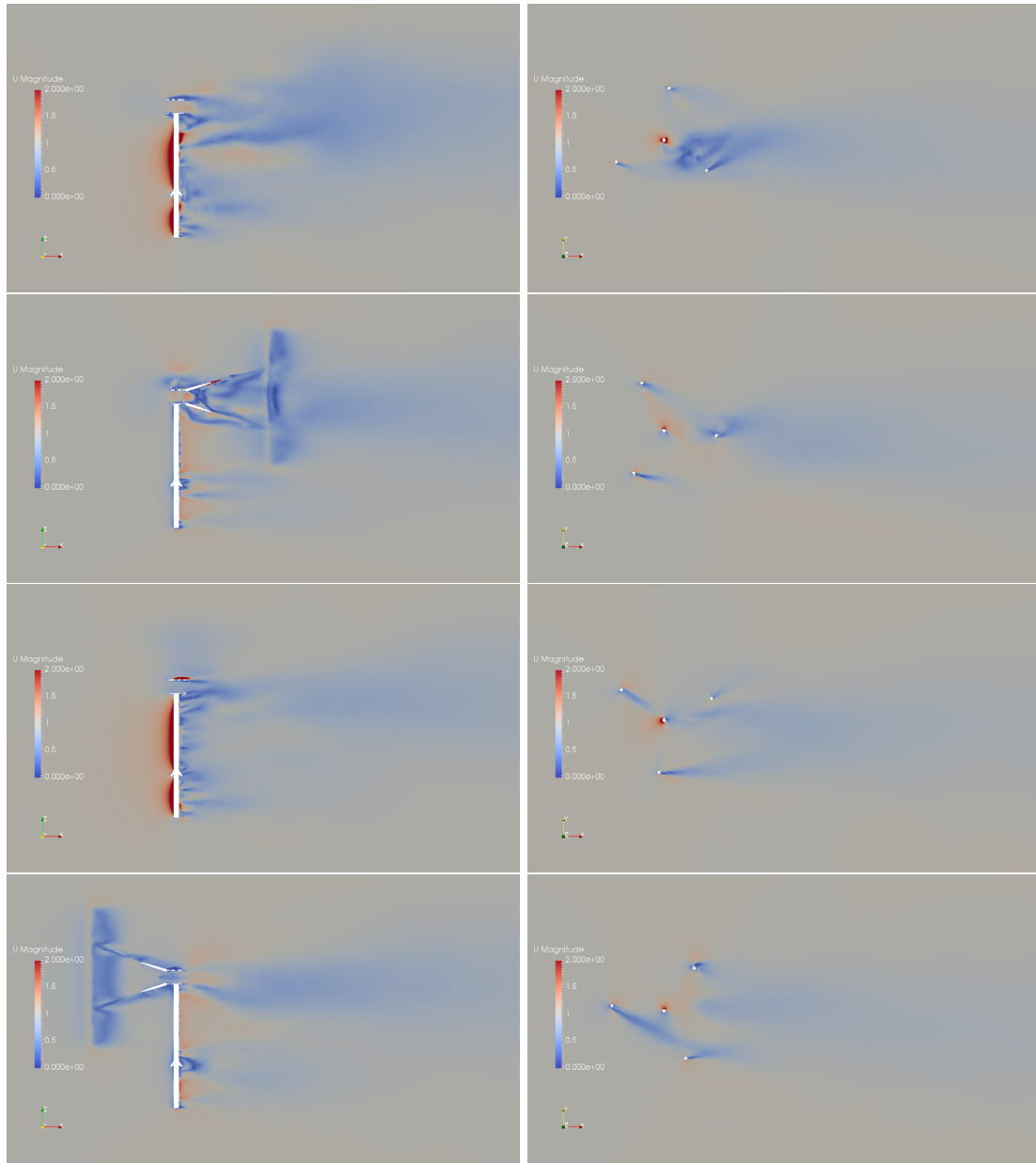


Figure 4: Rotating turbine at rotational speed $\pi/20$ rad/s, for 4 snapshots in time: horizontal cuts (left) and vertical cuts (right).

ACKNOWLEDGEMENTS

This research has been supported by the European Research Council, the Swedish Energy Agency, the Basque Excellence Research Center (BERC 2014-2017) program by the Basque Government, the Spanish Ministry of Economy and Competitiveness MINECO: BCAM Severo

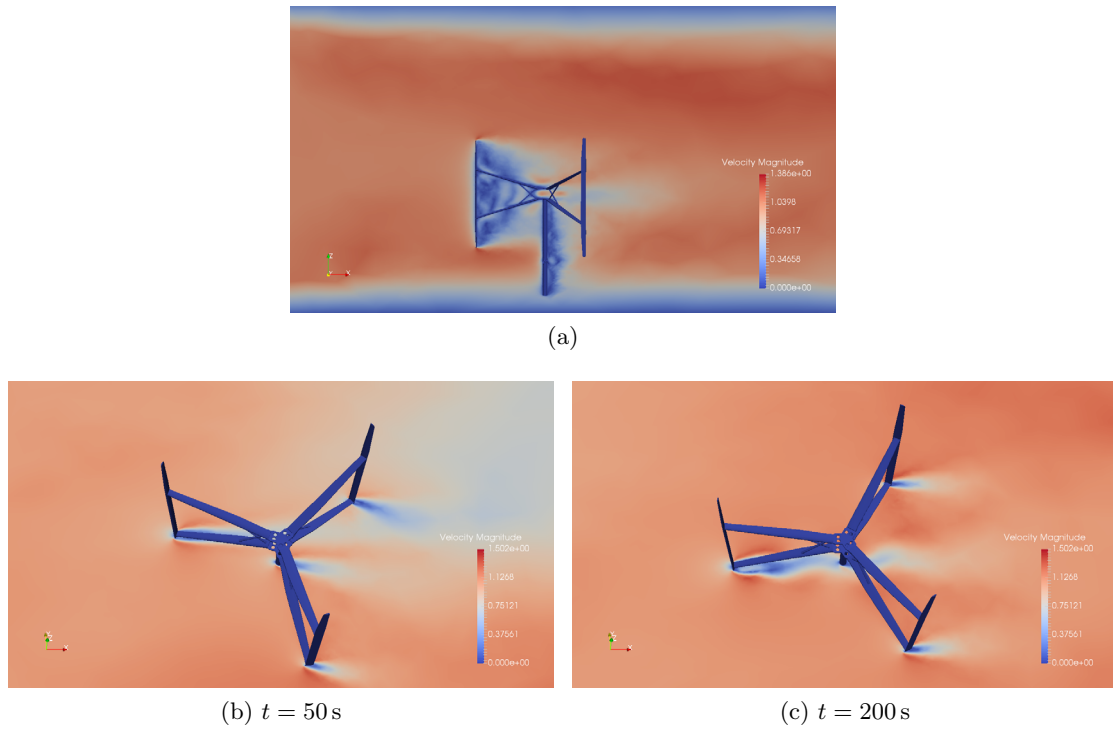


Figure 5: A vertical cut of the computed velocity (a). Under the effect of the inflow velocity, the turbine only rotates for a while (b) before stopping in the position shown in (c).

Ochoa accreditation SEV-2013-0323, the ICERMAR ELKARTEK project of the Basque Government, the Projects of the Spanish Ministry of Economy and Competitiveness with reference MTM2013-40824-P and MTM2016-76016-R. We acknowledge the Swedish National Infrastructure for Computing (SNIC) at PDC – Center for High-Performance Computing for awarding us access to the supercomputer resource Beskow. The initial volume mesh was generated with ANSA from Beta-CAE Systems S. A., who generously provided an academic license for this project.

REFERENCES

- [1] Anders Ahlström. Aerolastic simulation of wind turbine dynamics. 2005.
- [2] Y. Bazilevs, M.-C. Hsu, I. Akkerman, S. Wright, K. Takizawa, B. Henicke, T. Spielman, and T. E. Tezduyar. 3d simulation of wind turbine rotors at full scale. part i: Geometry modeling and aerodynamics. *International Journal for Numerical Methods in Fluids*, 65(1-3):207–235, 2011.
- [3] Y. Bazilevs, M.-C. Hsu, J. Kiendl, R. Wehner, and K.-U. Bletzinger. 3d simulation of wind turbine rotors at full scale. part ii: Fluidstructure interaction modeling with composite blades. *International Journal for Numerical Methods in Fluids*, 65(1-3):236–253, 2011.

- [4] Jean Donea, Antonio Huerta, Jean-Philippe Ponthot, et al. Arbitrary lagrangian eulerian methods. *Encyclopedia of Computational Mechanics*, 2004.
- [5] Eduard Dyachuk and Anders Goude. Numerical validation of a vortex model against experimental data on a straight-bladed vertical axis wind turbine. *Energies*, 8(10):11800–11820, 2015.
- [6] J. Hoffman and C. Johnson. Stability of the dual Navier-Stokes equations and efficient computation of mean output in turbulent flow using adaptive DNS/LES. *Computer Methods in Applied Mechanics and Engineering*, 195:1709–1721, February 2006.
- [7] Johan Hoffman, Johan Jansson, Rodrigo V. de Abreu, Cem Degirmenci, Niclas Jansson, Kaspar Müller, Murtazo Nazarov, and Jeanette H. Spühler. Unicorn: Parallel adaptive finite element simulation of turbulent flow and fluid-structure interaction for deforming domains and complex geometry. *Computer and Fluids*, in press, 2012.
- [8] Johan Hoffman, Johan Jansson, and Niclas Jansson. Fenics-hpc: Automated predictive high-performance finite element computing with applications in aerodynamics. In *11th International Conference on Parallel Processing and Applied Mathematics*. Springer-Verlag New York, 2015.
- [9] Johan Jansson, V. Nava, M. Sanchez, G. Aguirre, Rodrigo Vilela De Abreu, Johan Hoffman, and J. L. Villate. Adaptive simulation of unsteady flow past the submerged part of a floating wind turbine platform. In *MARINE 2015 - Computational Methods in Marine Engineering VI* :, pages 35–46, 2015. QC 20151125.
- [10] David A Spera. Wind turbine technology. 1994.